Inorganic Chemistry

Article

pubs.acs.org/IC

X-ray Diffraction, Mössbauer Spectroscopy, Magnetic Susceptibility, and Specific Heat Investigations of Na_4NpO_5 and Na_5NpO_6

Anna L. Smith,*[,†,‡] Amir Hen,[†] Philippe E. Raison,*[,†] Eric Colineau,[†] Jean-Christophe Griveau,[†] Nicola Magnani,[†] Jean-Pierre Sanchez,[§,∥] Rudy J. M. Konings,[†] Roberto Caciuffo,[†] and Anthony K. Cheetham[‡]

[†]European Commission, Joint Research Centre, Institute for Transuranium Elements, P.O. Box 2340, D-76125 Karlsruhe, Germany

[‡]Department of Materials Science and Metallurgy, University of Cambridge, 27 Charles Babbage Road, Cambridge CB3 0FS, United Kingdom

[§]CEA, INAC-SPSMS, FR-38000 Grenoble, France

[∥]Université de Grenoble Alpes, INAC-SPSMS, FR-38000 Grenoble, France

Supporting Information

ABSTRACT: The hexavalent and heptavalent sodium neptunate compounds Na_4NpO_5 and Na_5NpO_6 have been investigated using X-ray powder diffraction, Mössbauer spectroscopy, magnetic susceptibility, and specific heat measurements. Na_4NpO_5 has tetragonal symmetry in the space group $I4/m$, while Na_5NpO_6 adopts a monoclinic unit cell in the space group $C2/m$. Both structures have been refined for the first time using the Rietveld method. The valence states of neptunium in these two compounds, i.e., Np(VI) and Np(VII), respectively, have been confirmed by the isomer shift values of their Mössbauer spectra. The local structural properties obtained from the X-ray refinements have also been related to the quadrupole coupling constants and asymmetry parameters determined from the Mössbauer studies. The absence of magnetic ordering has been confirmed for Na_4NpO_5. However, specific heat measurements at low temperatures have suggested the existence of a Schottky-type anomaly at around 7 K in this Np(VI) phase.

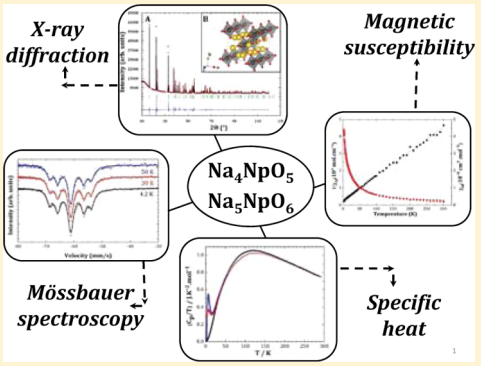

INTRODUCTION

The study of the ternary oxides of uranium, neptunium, and plutonium formed with sodium metal has been of great interest since the 1950s and 1960s because of their technological importance for sodium-cooled fast reactors (SFRs).[1] In the potential event of a breach of the stainless steel cladding, the sodium metallic coolant might indeed come into contact with the $(U,Np,Pu)O_2$ nuclear fuel, leading to the formation of such ternary phases. The knowledge of their structural, thermomechanical, and thermodynamic properties is therefore essential from safety perspectives. Keller and his co-workers are the pioneers of the studies on the interaction between alkali metals and the actinide elements (Np,Pu,Am).[2,3] Using various synthesis routes, the authors reported the formation of pentavalent Na_3NpO_4,[3] as well as hexavalent $Na_2Np_2O_7$, Na_2NpO_4, Na_4NpO_5, and Na_6NpO_6.[2] The corresponding structures were determined using the Debye−Scherrer method. A number of space groups could not be determined at that time, however, and uncertainties remained. As part of a program of research at the Joint Research Centre-Institute for Transuranium Elements (JRC-ITU, Karlsruhe, Germany), the structural properties of the Na−Np−O ternary phases are currently being reinvestigated.[4]

In addition, these ternary compounds containing a $[Rn]5f^n$ central ion have also attracted considerable attention because of their interesting electronic and magnetic properties.[5−7] For actinide oxide compounds, the crystal-field interaction is usually of the same order of magnitude as the spin−orbit coupling interaction and electronic repulsion,[8] which makes the interpretation very complex. As the 5f-orbitals of the actinides have a much greater radial extension than the 4f-orbitals of the lanthanides, which are more core-like, the crystal-field interaction cannot be treated as a small perturbation of the electronic energy levels as is done for $[Xe]4f^n$ rare earths.[8] In the case of $[Rn]5f^1$ and $[Rn]5f^0$ electronic configurations, however, corresponding to hexavalent and heptavalent neptunium, respectively, the contribution from electronic repulsion is removed, which greatly simplifies the interpretation.

In the present work, we report structural refinements for hexavalent Na_4NpO_5 and heptavalent Na_5NpO_6 using the Rietveld method, as well as their coefficients of thermal expansion derived from high temperature X-ray diffraction measurements. X-ray diffraction gives information on the

Received: February 26, 2015
Published: April 10, 2015

DOI: 10.1021/acs.inorgchem.5b00462
Inorg. Chem. 2015, 54, 4556−4564

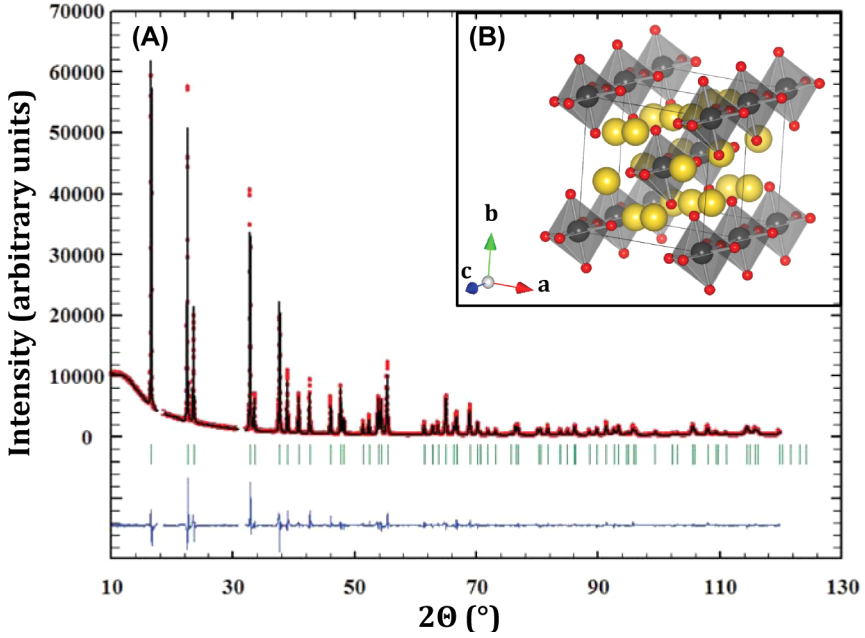

Figure 1. (A) Comparison between the observed (Y_{obs}, in red) and calculated (Y_{calc}, in black) X-ray diffraction pattern of Na_4NpO_5. $Y_{obs} - Y_{calc}$, in blue, is the difference between the experimental and calculated intensities. The Bragg reflections' angular positions are marked in green. Measurement at λ = Cu Kα1. (B) The inset shows the crystal structure of Na_4NpO_5 (Na atoms in yellow, O atoms in red, NpO_6 octahedra in gray) showing the chains along c of corner sharing NpO_6 octahedra.

structures, but it cannot provide a definitive signature of the oxidation state of the neptunium ion in those compounds. ^{237}Np Mössbauer spectroscopy is a very powerful technique for this purpose, which is used herein to confirm the respective Np(VI) and Np(VII) valence states in Na_4NpO_5 and Na_5NpO_6. It also gives a direct insight into the electronic and local structural environment around the Np nucleus, as well as the magnetic field acting on it.[9] The local environment around the neptunium ion is therefore also discussed in this study with respect to the fitted Mössbauer parameters, i.e., quadrupole coupling constants and asymmetry parameters. Moreover, the absence of magnetic ordering is confirmed for both compositions. Finally, specific heat measurements of Na_4NpO_5 are reported, which show a broad Schottky-type anomaly around 7 K. Explanations for this feature are suggested.

EXPERIMENTAL METHODS

Sample Preparation. Na_4NpO_5 and Na_5NpO_6 were synthesized by grinding together stoichiometric amounts of neptunium dioxide ($^{237}NpO_2$ from JRC-ITU stocks, provided by ORNL, Oak Ridge National Laboratory) and sodium carbonate (Na_2CO_3 99.95%, Sigma), and heating the mixtures at 1100 K for 60−70 h under oxygen flow with intermediate regrinding steps. Two different batches of Na_4NpO_5 material were prepared. The former, used for Mössbauer spectroscopy and magnetic susceptibility measurements, contained 1.8 wt % of Na_5NpO_6 impurity, while the latter, used for specific heat measurements at low temperatures, showed 0.5 wt % of α-Na_2NpO_4 impurity. The characterization of the sample's purity for the specific heat measurement was reported in detail in another publication,[10] and the collected data were corrected for the α-Na_2NpO_4 contribution. As for the Na_5NpO_6 material, no secondary phases were detected by X-ray diffraction.

^{237}Np decays to ^{233}Pa by α emission with a half-life of 2.14 million years. The ^{233}Pa daughter product is a β^- emitter with a very short half-life (27 days) and significant γ dose rate [1.335×10^{-4} (mSv/h)/MBq].[11] Therefore, the handling of the neptunium samples, which requires great safety precautions, was done with limited quantities in nitrogen-filled α-gloveboxes.

X-ray Powder Diffraction. The samples were characterized at room temperature by X-ray diffraction using a Bruker D8 Bragg−Brentano X-ray diffractometer mounted inside a glovebox and equipped with a curved Ge monochromator (111), a ceramic copper tube (40 kV, 40 mA), and a LinxEye position sensitive detector. The data were collected by step scanning in the range $10° \leq 2\theta \leq 120°$, with an integration time of about 8 h, a count step of 0.02° (2θ), and a dwell of 5 s/step. Structural analysis was performed by the Rietveld method using the Fullprof2k suite.[12]

The thermal expansion and stability of the Na_4NpO_5 and Na_5NpO_6 phases were also assessed by high temperature X-ray diffraction using the same diffractometer equipped with an Anton Paar HTK 2000 chamber. Measurements were conducted under helium up to 1273 K. The heating chamber was purged several times before the experiment and filled to about 600−700 mbar. The temperature, measured with a thermocouple, was previously calibrated using the thermal expansion data of MgO.[13] The uncertainty on the temperature is estimated to be 20 K at 1473 K.

Mössbauer Spectroscopy. The ^{237}Np Mössbauer measurements were carried out in transmission, using an ^{241}Am metal source with a sinusoidal driving mode. The effect was measured with a photon energy of 59.54 keV. The Na_4NpO_5 and Na_5NpO_6 powder samples, encapsulated in 3 concentric aluminum containers, were measured in the temperature ranges 4.2−20 and 4.2−50 K, respectively, while the source was kept at a constant temperature of 4.2 K inside a stainless steel cryostat.

Magnetic Susceptibility Measurements. Magnetic susceptibility measurements were made using a SQUID magnetometer (Quantum Design MPMS-7) from 3 to 301 K, in a field of B = 1 T, on a 19.90(5) mg Na_4NpO_5 sample encapsulated in Stycast 2850 FT. The contribution of the Stycast was subtracted from the recorded data.

Specific Heat Investigations. Low temperature heat capacity measurements were performed on the Na_4NpO_5 material using a PPMS (Physical Property Measurement System, Quantum Design) instrument, in the absence of a magnetic field in the temperature range

DOI: 10.1021/acs.inorgchem.5b00462
Inorg. Chem. 2015, 54, 4556−4564

2.4−292.2 K, and in a 7, 10, and 14 T magnetic field in the temperature range 2.4−20.4 K.

The PPMS technique is based on a relaxation method, which was critically assessed by Lashley et al.[14] The measurements were carried out on 21.07(5) mg of Na_4NpO_5 material encapsulated in Stycast 2850 FT, and the heat capacity contribution of the Stycast was subtracted from the recorded data. A more detailed description of the experimental procedure, which is particularly well-adapted to the study of radioactive materials, was given in ref 15. The contributions from the sample platform, wires, and grease were also deduced by a separate measurement of an addenda curve. On the basis of the experience acquired on this instrument with standard materials and other compounds,[14,15] the uncertainty was estimated at about 1% in the middle range of acquisition, and reached about 3% at the lowest temperatures and near room temperature.

RESULTS AND DISCUSSION

X-ray Powder Diffraction. Na_4NpO_5 was reported to be isostructural with Na_4UO_5, i.e., tetragonal in the space group $I4/m$ by Smith et al.,[4] but the quality of the latter X-ray data was not good enough to perform a Rietveld refinement. A new synthesis route using sodium carbonate instead of sodium oxide led to a more crystalline sample in the present work, allowing the determination of the structure. The X-ray diffraction pattern for Na_4NpO_5 is shown in Figure 1A. The refined cell parameters are a = 7.535(3) Å, c = 4.616(3) Å. The atomic positions are listed in Table 1, and selected bond lengths are given in the Supporting Information.

Table 1. Refined Atomic Positions in Na_4NpO_5[a]

atom	ox. state	Wyckoff	x	y	z	B_0 (Å^2)
Na	+1	8h	0.198(1)	0.403(1)	0	0.85(1)
Np	+6	2a	0	0	0	0.25(1)
O1	−2	2b	0	0	0.5	2.49(1)
O2	−2	8h	0.259(1)	0.083(1)	0	1.88(1)

[a] R_{wp} = 17.7%, R_{exp} = 4.45%, χ^2 = 15.9 (standard deviation = 3σ). 5578 points for pattern. 82 refined parameters. Peak shape η: Pseudo-Voigt axial divergence asymmetry. Background: Linear interpolation between operator-selected points in the pattern. The rather large value of R_{wp} comes from an asymmetric profile in opposite directions for successive hkl reflections, which is particularly pronounced at low angles (as shown in the Supporting Information). This is due to slight heterogeneity within the material which creates constraints. It was not possible to improve the refinement using the reflection profile functions of the Fullprof software.

The structure is made of "reverse" neptunyl type of NpO_6 octahedra, with two long Np−O(1) bonds at 2.31(1) Å along the axial c direction, and four short Np−O(2) bonds at 2.05(1) Å in the equatorial ab plane, as shown in Figure 2. By contrast, a $(NpO_2)^{2+}$ neptunyl type of configuration consists of two close oxygen neighbors in the axial direction and four distant ones in the equatorial plane. The NpO_6 octahedra in Na_4NpO_5 exhibit perfect axial symmetry, which is important information for the Mössbauer study. Moreover, they share corners between each other forming parallel and infinite chains in the c direction, with a Np−O(1)−Np angle of 180° (Figure 1B). The intrachain Np−Np distance is 4.62(1) Å, and the interchain Np−Np distance is large (5.81(1) Å). The chains can hence be considered as well-isolated from a magnetic point of view. This particular type of reverse neptunyl configuration is unique among the series of sodium neptunate compositions,[4] and unusual among the larger family of alkali metal−actinide ternary oxide phases. It is found in the isotructural Na_4UO_5[16] and Li_4NpO_5 compounds.[17] This specific feature is probably related to the Np−O−Np arrangement in chains. As for the sodium atoms, they are located between the chains, and bind them together. The NaO_6 octahedra are rather distorted with Na−O bond lengths covering the range 2.33(1)−2.69(1) Å. Finally, the unit cell volume of Na_4NpO_5 (262.1 Å^3) is slightly smaller than the unit cell volume of the isostructural Na_4UO_5 compound (264.2 Å^3),[18] which is consistent with the ionic radii for Np^{6+} (0.72 Å) and U^{6+} (0.73 Å) according to Shannon's tabulated data.[19]

The present X-ray diffraction pattern for Na_5NpO_6, shown in Figure 3, was refined using monoclinic Li_5ReO_6, in space group $C2/m$, as a starting model,[20] leading to the cell parameters a = 5.829(3) Å, b = 9.996(3) Å, c = 5.757(3) Å, and β = 110.73(1)°. Refined atomic positions are given in Table 2. Keller et al. first reported in 1965 the formation of Na_6NpO_6 by reaction at 723 K between sodium oxide and neptunium oxide mixed in a (3:1) ratio,[2,4] and identified the compound as isostructural with Li_6ReO_6, but did not perform Mössbauer spectroscopy to confirm the Np(VI) valence state.[21] Reproducing the synthesis conditions of Keller et al.,[2] Smith et al. have shown that the compound formed was most probably heptavalent Na_5NpO_6, rather than hexavalent Na_6NpO_6.[4] The sample prepared in this work with sodium carbonate instead of sodium oxide is a nicely crystalline forest green material, of sufficient quality for the determination of the structure.

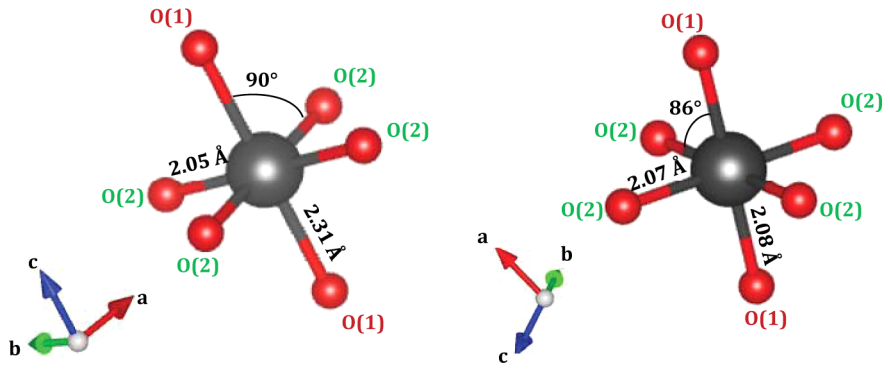

(a) Na_4NpO_5 (b) Na_5NpO_6

Figure 2. Sketch of the NpO_6 octahedra in Na_4NpO_5 and Na_5NpO_6.

DOI: 10.1021/acs.inorgchem.5b00462
Inorg. Chem. 2015, 54, 4556−4564

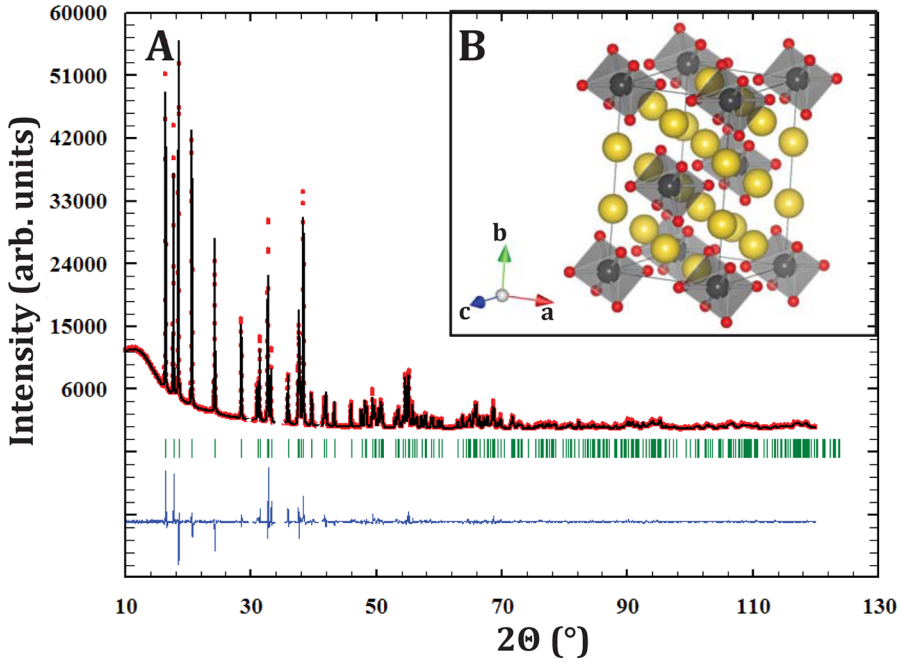

Figure 3. (A) Comparison between the observed (Y_{obs}, in red) and calculated (Y_{calc}, in black) X-ray diffraction pattern of Na_5NpO_6. $Y_{obs} - Y_{calc}$, in blue, is the difference between the experimental and calculated intensities. The Bragg reflections' angular positions are marked in green. Measurement at λ = Cu Kα1. (B) The inset shows the crystal structure of Na_5NpO_6 (Na atoms in yellow, O atoms in red, NpO_6 octahedra in gray) showing the isolated NpO_6 octahedra.

Table 2. Refined Atomic Positions for the Na_5NpO_6 Phase[a]

atom	ox. state	Wyckoff	x	y	z	B_0 (Å^2)
Np	+7	2a	0	0	0	0.66(1)
Na1	+1	4g	0	0.664(1)	0	0.29(1)
Na2	+1	2d	0	0.5	0.5	0.29(1)
Na3	+1	4h	0.5	0.330(1)	0.5	0.29(1)
O1	−2	4i	0.267(1)	0.5	0.202(1)	1.56(1)
O2	−2	8j	0.271(1)	0.354(1)	0.784(1)	1.56(1)

[a] R_{wp} = 13.7%, R_{exp} = 3.95%, χ^2 = 12.1 (standard deviation = 3σ). 5578 points for pattern. 84 refined parameters. Peak shape η: Pseudo-Voigt axial divergence asymmetry. Background: Linear interpolation between operator-selected points in the pattern.

Table 3. Selected Bond Lengths, R (Å), and Angles for Na_5NpO_6 Derived from the X-ray Diffraction Data[a]

bond	N	R (Å)
Np−O(1)	2	2.08(1)
Np−O(2)	4	2.07(1)
Na(1)−O(1)	2	2.28(1)
Na(1)−O(2)	2	2.34(1)
Na(1)−O(2)	2	2.40(1)
Na(2)−O(1)	2	2.69(1)
Na(2)−O(2)	4	2.34(1)
Na(3)−O(1)	2	2.45(1)
Na(3)−O(2)	2	2.46(1)
Na(3)−O(2)	2	2.60(1)
angle		deg
O(1)−Np−O(1)		180
O(2)−Np−O(2)		180
O(2)−Np−O(1)		85.8(1)

[a] Standard deviations are given in parentheses. N is the number of atoms in each coordination shell.

The structure of Na_5NpO_6, in contrast with that of Na_4NpO_5, comprises isolated NpO_6^{5-} octahedra in association with charge-compensating Na^+ cations. Selected bond lengths and bond angles are listed in Table 3. The NpO_6 octahedra have two axial Np−O(1) bonds at 2.08(1) Å and four equatorial Np−O(2) bonds at 2.07(1) Å, as shown in Figure 2. The axial O(1)−Np−O(1) bond is moreover slightly tilted with respect to the equatorial plane [with an O(1)−Np−O(2) angle of 85.8(1)°]. This feature is of importance for the interpretation of the Mössbauer data as detailed in the next section. As for the NaO_6 octahedra, they are rather distorted (with minimum and maximum bond lengths 2.28(1) and 2.69(1) Å, respectively). The unit cell volume of isostructural Na_5PuO_6 synthesized by a very similar procedure,[22] i.e., 312.6 Å^3, is slightly smaller than that of Na_5NpO_6 (313.8 Å^3), which is consistent with a smaller ionic radius of Pu^{7+} compared to that of Np^{7+}.

Mössbauer Spectroscopy. The Mössbauer spectra of Na_4NpO_5 recorded at 4.2 and 20 K are shown in Figure 4. They both consist of a broad line due to an unresolved axial (asymmetry parameter η = 0) quadrupole interaction, whose quadrupole coupling constant amounts to $|e^2qQ|$ = 10.5(3) mm s^{-1}. The isomer shift is δ_{IS} = −53.5(3) mm s^{-1} with respect to $NpAl_2$. Its value lies in the range −32 > δ_{IS} > −62 mm s^{-1}, confirming the Np(VI) charge state in Na_4NpO_5, corresponding to a [Rn]5f^1 electronic configuration, as displayed in the correlation diagram in the Supporting Information. The Np ion in this structure is therefore a Kramers ion with a $^2F_{5/2}$ ground state manifold and $^2F_{7/2}$ first excited state arising from spin−orbit coupling. The investigated material contains a small impurity, however, which manifests itself in the form of a broad line centered at −61.0 mm s^{-1}, corresponding to an isomer shift of δ_{IS} = −74.6(3) mm s^{-1} versus $NpAl_2$. The latter impurity was identified as Na_5NpO_6 from the X-ray diffraction pattern (1.8 wt %), and estimated to represent about 7% of the

DOI: 10.1021/acs.inorgchem.5b00462
Inorg. Chem. 2015, 54, 4556−4564

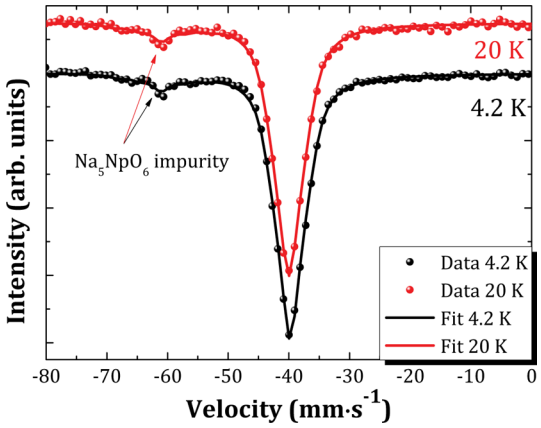

Figure 4. Mössbauer spectra of Na_4NpO_5 recorded at 4.2 and 20 K.

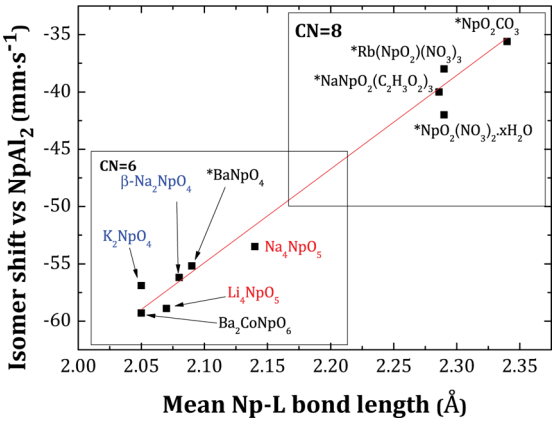

Figure 5. Isomer shift versus mean neptunium−ligand (Np−L) distance for selected hexavalent neptunium compounds with coordination numbers (CNs) 6 and 8. The red line is a linear fit of the experimental points. Asterisk indicates that, when not available, the mean (Np−L) distance was approximated with the mean (U−L) distance reported by Jové et al.[23] and was corrected for the difference in ionic radius between Np^{6+} and U^{6+} according to Shannon's tabulated data,[19] i.e., 0.01 Å.

total sample from the relative areas of the two subspectra. There is no change in the spectral shape between 4.2 and 20 K, except for a slight decrease in overall intensity with increasing temperature, which was attributed to the temperature dependence of the Lamb−Mössbauer factor. Thus, we can exclude the occurrence of a magnetic phase transition within the probed temperature range.

It is interesting to compare the present fitted Mössbauer parameters with those for Li_4NpO_5, K_2NpO_4, and β-Na_2NpO_4 listed in Table 4. The NpO_6 octahedra for all four compounds show axial symmetry so that $\eta = 0$. The local symmetry around the neptunium ion in Li_4NpO_5 is also a reverse neptunyl type of configuration, and both compounds, Na_4NpO_5 and Li_4NpO_5, have similar values of the quadrupole coupling constant $|e^2qQ|$, 10.5 and 18 mm s^{-1}, respectively, which originates from the slight axial elongation of the NpO_6 octahedra. By contrast, K_2NpO_4 and β-Na_2NpO_4, which both contain the $(NpO_2)^{2+}$ neptunyl type of ions, have quadrupole coupling constant values around 100 mm s^{-1}.

Jové et al., who have investigated correlations among the isomer shift, electric field gradient, and local neptunium structure in crystallized and amorphous neptunium compounds covering the Np(III) to Np(VII) valence states,[23,24] have pointed out the existence of a linear relationship between the average neptunium−ligand distance and isomer shift for hexavalent neptunium compounds.[23,24] The values reported herein for Na_4NpO_5 fit very well with this trend, as shown in Figure 5. The Np−O mean values of Li_4NpO_5,[17] K_2NpO_4,[22] β-Na_2NpO_4,[4,26] and Ba_2CoNpO_6[28,29] have been updated in this figure compared to the values in the figure of Jové et al.[24] The authors also have emphasized a correlation between the values of the quadrupole coupling constant $|e^2qQ|$ and isomer shift, with a separate region for the non-neptunyl compounds NpF_6, Ba_2CoNpO_6, Ba_2CuNpO_6, and Li_4NpO_5.[24] The Mössbauer parameters found herein for Na_4NpO_5 satisfy the criteria for this group of compounds, i.e., $0 < |e^2qQ| < 50$ mm s^{-1} and $-63 < \delta_{IS} < -52$ mm s^{-1}.

As for Na_5NpO_6, the Mössbauer spectra recorded at 4.2, 30, and 50 K, and shown in Figure 6, consist of a single quadrupolar split pattern centered at −61.2 mm s^{-1}, which corresponds to an isomer shift of $\delta_{IS} = -74.8(3)$ mm s^{-1} relative to the standard $NpAl_2$ absorber. This shift confirms the Np(VII) valence state. Np(VII) is indeed found in an isomer shift range $-60 < \delta_{IS} < -78$ mm s^{-1} according to the correlation diagram in the Supporting Information. Its value is significantly less negative than the free ion Np^{7+} value estimated to be −194 mm $s^{-1}/NpAl_2$.[6] This reveals large partial occupation of the bonding orbitals by the 5f and 6d electrons.[30]

The measured data were fitted using a quadrupole coupling constant $|e^2qQ|$ of 25.9(3) mm s^{-1}, and an asymmetry parameter η (affecting the external line positions) of 0.43(3). A slight decrease in overall intensity was observed with increasing temperature, as expected from the temperature dependence of the Lamb−Mössbauer factor.

The Mössbauer parameters found herein are compared in Table 5 to the values reported in the literature for Na_5NpO_6

Table 4. Structural and Mössbauer Parameters for Some Alkali Oxo-Neptunates

compd	bond lengths (Å)	ref	δ_{IS} (mm $s^{-1}/NpAl_2$)	$\lvert e^2qQ\rvert$ (mm s^{-1})	η	H_{hf} (T)	ref
Na_4NpO_5	$Np-O_I$ = 2.06 (×4)	*a*	−53.5(3)[b]	10.5(3)	0		*a*
	$Np-O_{II}$ = 2.31 (×2)						
Li_4NpO_5	$Np-O_I$ = 2.00 (×4)	17	−58.9(3)[c]	18	0		23, 24
	$Np-O_{II}$ = 2.21 (×2)						
K_2NpO_4	$Np-O_I$ = 1.84 (×2)	22	−56.9(6)[c]	88	0	122[d]	23, 25
	$Np-O_{II}$ = 2.15 (×4)						
β-Na_2NpO_4	$Np-O_I$ = 1.90 (×2)	4, 26	−56.2(3)[c]	103.2(3)	0		27
	$Np-O_{II}$ = 2.16 (×2)						
	$Np-O_{III}$ = 2.17 (×2)						

[a]Present work. [b]IS value at 4.2 K. [c]IS value at 77 K. [d]Updated value for the ground state nuclear moment, μ_g = 2.5 nm.

DOI: 10.1021/acs.inorgchem.5b00462
Inorg. Chem. 2015, 54, 4556−4564

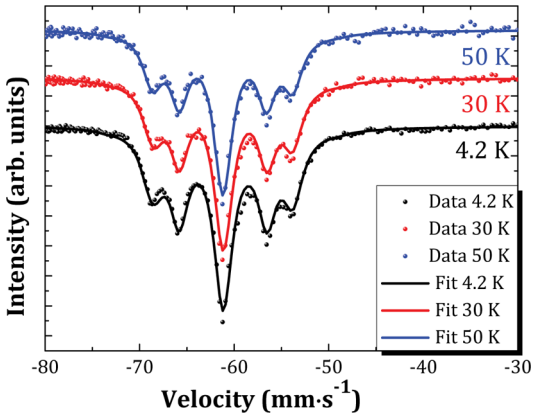

Figure 6. Mössbauer spectra of Na_5NpO_6 recorded at 4.2, 30, and 50 K.

Table 5. Mössbauer Parameters for Some Alkali Heptavalent Neptunates

compd	δ_{IS} (mm s^{-1}/$NpAl_2$)	$\lvert e^2qQ\rvert$ (mm s^{-1})	η	ref
Na_5NpO_6	−74.8(3)[b]	25.9(3)	0.43(3)	*a*
Na_5NpO_6	−75.7[b]	24	1	24
Li_5NpO_6	−78(2)[b]	34(1)	0.34(3)	35
Li_5NpO_6	−74.8(29)[b]	32.9(8)	0.33(1)	36
Li_5NpO_6	−77.2(3)[b]	35(1)	0.30(5)	30

[a]Present work. [b]IS value at 4.2 K.

and Li_5NpO_6. Jov et al. mentioned Mössbauer parameters for Na_5NpO_6,[24] but the corresponding spectrum was, to the authors' knowledge, never published.[31] The isomer shift and quadrupole coupling constant reported, i.e., δ_{IS} = −75.7 mm s^{-1} and $\lvert e^2qQ\rvert$ = 24 mm s^{-1}, are very similar to ours, but the asymmetry parameter given by them, η = 1, would correspond to a spectrum with three lines only. This does not correspond to our experimental observation of a quintet. The structure of Li_5NpO_6 is still a subject of controversy.[17,32−34] The most recent study by Morss et al., who performed neutron diffraction studies on this compound,[17] points toward the monoclinic *C*2/*m* model of Li_5ReO_6, but a set of six weak reflections remains unidentified. The three sets of Mössbauer parameters reported for Li_5NpO_6 are nevertheless in good agreement as shown in Table 5.

In both cases, i.e., Na_5NpO_6 and Li_5NpO_6, the existence of a quadrupole coupling constant $\lvert e^2qQ\rvert$, and nonvanishing asymmetry parameter η, indicates a symmetry lower than O_h. Our X-ray refinement indicates that the O(1)−Np−O(1) axis is tilted by 4° with respect to the equatorial plane (with an O(1)−Np−O(2) angle of 86°), which could explain the presence of an asymmetry parameter. The observed quadrupolar interaction appears to be essentially due to the occupation of the bonding orbitals.[30] A neutron diffraction study would be required for a more accurate estimation of the Np−O distances and the exact geometry of the NpO_6 octahedra. However, by comparison with the data for Li_5NpO_6, we can suspect a distortion in Na_5NpO_6 more pronounced than that in Li_5NpO_6.

Finally, looking at general trends among heptavalent neptunium compounds, Friedt et al. reported an increasing linear variation of the quadrupole coupling constant as a function of isomer shift[30,37] through the series of compounds Li_5NpO_6, Cs_3NpO_5, Rb_3NpO_5, $CsNpO_4$, and $RbNpO_4$, which was related to the increasing occupation of the 5f and 6d atomic orbitals. The parameters reported by Jové et al. for Ba_2NaNpO_6 and K_3NpO_5,[24] and those found herein for the Na_5NpO_6 compound, fit this trend very well as shown in Figure 7.

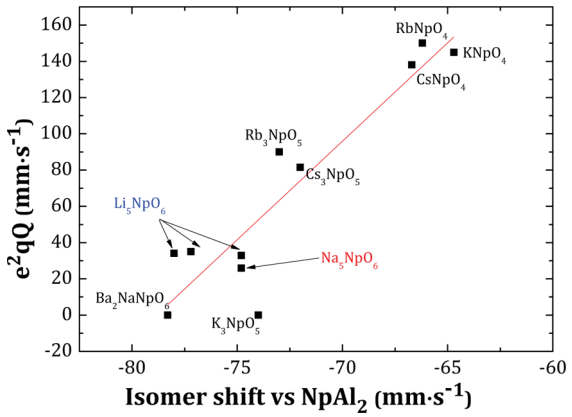

Figure 7. Variation of the isomer shift with respect to the quadrupole interaction for heptavalent neptunates. The red line is a linear fit of the experimental points.

Magnetic Susceptibility Studies of Na_4NpO_5. The magnetic susceptibility $\chi_M(T)$ data of Na_4NpO_5 exhibits paramagnetic behavior from room temperature down to 3 K (Figure 8): No anomaly is observed, confirming the absence of a magnetic ordering transition in this temperature range, in agreement with previous studies of Bickel et al.[38] and the present Mössbauer results.

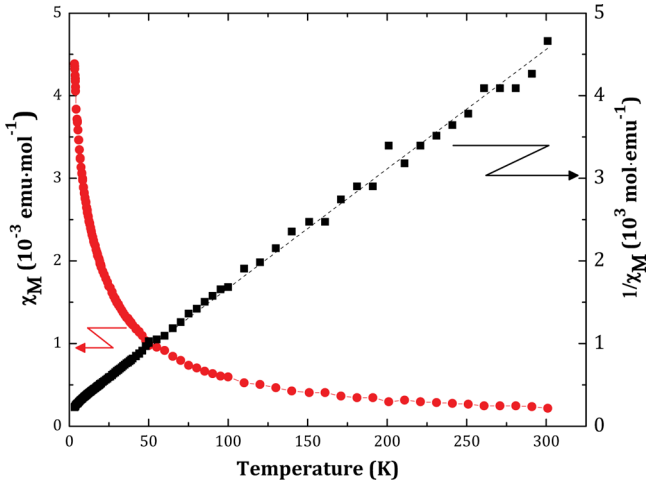

Figure 8. Magnetic suceptibility of Na_4NpO_5 (red ●) and inverse susceptibility (black ■) as a function of temperature measured at B = 1 T. The dashed line shows the Curie−Weiss fit on the present data.

The inverse susceptibility curve $1/\chi_M(T)$ is linear and obeys a Curie−Weiss law with $C = 6.92(2) \times 10^{-2}$ emu K mol^{-1} and θ_p = −15.6(3) K. Although this compound does not order magnetically, the negative value of the Curie temperature suggests the presence of antiferromagnetic interactions. The effective moment inferred from the fit, $\mu_{eff} = 0.74(4)\mu_B$, is significantly smaller than the value expected for the free Np^{6+} ion (2.54 μ_B in Russell−Saunders coupling using the free-ion *J*-value of the ground $^2F_{5/2}$ multiplet, $g_J = {}^6/_7$). This lower value is typical for alkali metal−actinide ternary oxides with a [Rn]5f[1]

DOI: 10.1021/acs.inorgchem.5b00462
Inorg. Chem. 2015, 54, 4556−4564

central ion,[5] where ligand field effects are as important as spin−orbit effects.

Specific Heat Investigation of Na_4NpO_5. The low temperature heat capacity measurements of Na_4NpO_5 have revealed the existence of a broad anomaly between 3 and 15 K, which was moreover slightly shifted to lower temperatures when a magnetic field was applied, as shown in Figure 9.

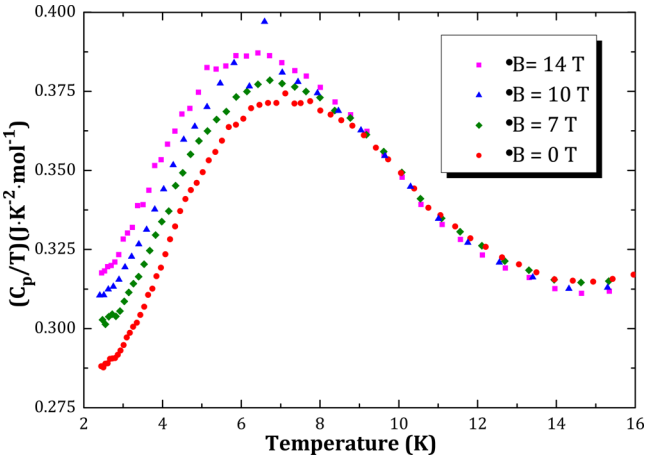

Figure 9. Evolution of the specific heat of Na_4NpO_5 with magnetic field.

The excess electronic contribution to the heat capacity was derived hereafter in an attempt to obtain better insight into the origin of the anomaly. The lattice contribution to the heat capacity of Na_4NpO_5 was approximated with that of the isostructural compound Na_4UO_5, with the electronic configuration $[Rn]5f^0$, reported in another publication.[10] The excess electronic heat capacity obtained from the difference between these two data is shown in Figure 10. Above 35 K, this electronic heat capacity becomes slightly negative, but this is insignificant considering the accuracy of the measurement. The heat capacity curves of Na_4UO_5 and Na_4NpO_5 cross around 60 K as can be seen in Figure 12, although we would expect the same lattice contribution for both compounds. This discrepancy can be related on the one hand to the uncertainty for our

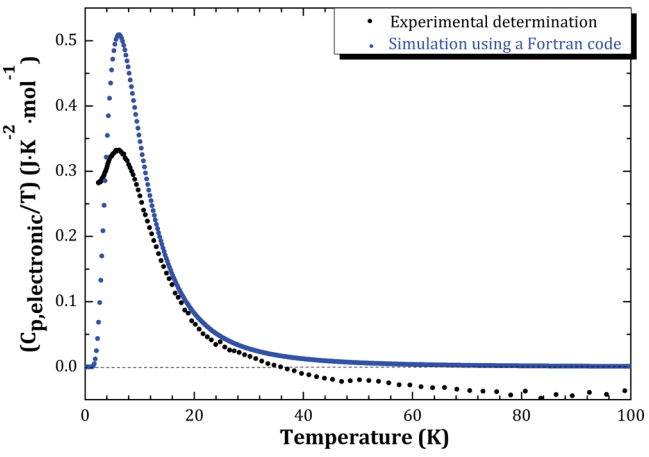

Figure 10. Electronic contribution to the heat capacity in Na_4NpO_5 obtained by subtracting the data of Na_4UO_5[10] (black ●), and comparison with the simulation for energy levels at 0, 14, 5910 cm^{-1} (blue ●) using a homemade Fortran code.

experimental results, which increases toward high temperatures using the PPMS technique, and on the other hand to the correction for the Stycast contribution.

The electronic entropy contribution could arise from an insulator−metal transition, a magnetic order−disorder transition, or a Schottky-type transition associated with crystal-field splitting of the energy levels.[39] The present Mössbauer measurements performed below and above the temperature of this anomaly, as well as the magnetic susceptibility measurements, have excluded the possibility of a magnetic ordering transition at this temperature. Furthermore, an insulator−metal transition is ruled out as Na_4NpO_5 is a lime green insulating material. The specific heat anomaly must hence be due to a Schottky-type behavior arising from low lying electronic energy levels. Its broad shape also resembles a Schottky-type feature rather than the λ peak associated with magnetic ordering. The numerical integration of the $(C_{p,electronic}/T) = f(T)$ curve in the temperature range 0−35 K using the OriginLab software yielded $S_{electronic}(Na_4NpO_5, 298.15\ K) = 4.57\ J\ K^{-1}\ mol^{-1}$, i.e., about 79% of the expected order−disorder entropy for such a Kramers system (R ln 2).

The electronic levels associated with the $^2F_{5/2}$ ground state were simulated using a homemade Fortran code in an attempt to reproduce the experimental results. The $^2F_{5/2}$ ground state has a degeneracy of $(2J + 1) = 6$, and is therefore split into three Kramers doublets (Γ_7 ground state, and Γ_7^t, Γ_6^t excited states) by the crystal-field effect in the tetragonally distorted (D_{4h}) symmetry,[5] as shown in the splitting scheme in Figure 11. The $^2F_{7/2}$ excited state is split in four Kramers doublets.

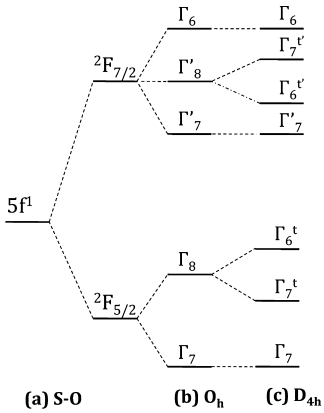

Figure 11. Splitting of the $5f^1$ electronic state by (a) spin−orbit coupling, (b) an O_h symmetry, and (c) a D_{4h} symmetry crystal field.[38]

Figure 10 compares the experimental electronic heat capacity with the one calculated for two low lying states having the same degree of electronic degeneracy and separated by 14 cm^{-1}. In Figure 12, the heat capacity of Na_4NpO_5 is moreover compared with the sum of the lattice contribution of Na_4UO_5 and excess electronic entropy calculated with the Fortran code. The agreement is rather good, which makes quite a strong case for the existence of a Schottky-type feature. Two configurations can be envisaged which reproduce these results: one where the Γ_7 ground state doublet is split itself by 14 cm^{-1}, the other one where the Γ_7^t or Γ_6^t doublet is found 14 cm^{-1} above the Γ_7 ground state doublet.

The splitting of the lowest electronic doublet by long-range magnetic ordering was already excluded on the basis of the susceptibility and Mössbauer data. Another explanation for a Γ_7

DOI: 10.1021/acs.inorgchem.5b00462
Inorg. Chem. 2015, 54, 4556−4564

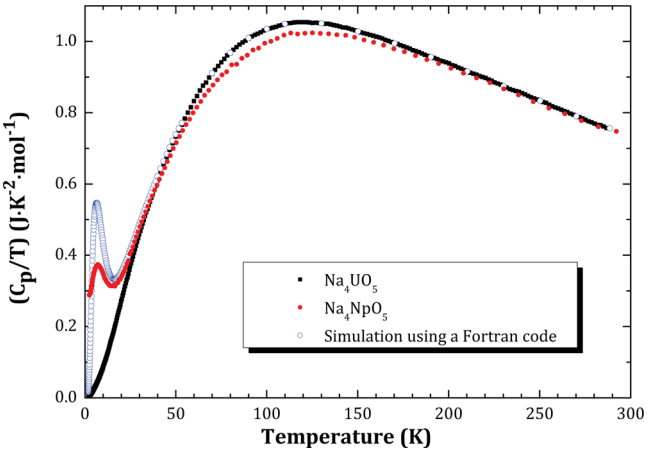

Figure 12. C_p/T for Na_4UO_5 (black ■) and Na_4NpO_5 (red ●) measured in zero magnetic field, and comparison with the sum of the lattice contribution of Na_4UO_5 and excess electronic entropy obtained by simulating energy levels at 0, 14, 5910 cm^{-1} (blue ○) using a homemade Fortran code.

ground state splitting would be the occurrence of hyperfine interactions with the $I = {}^5/_2$ nuclear spin of ^{237}Np. Considering that the crystal-field potential of the reverse neptunyl geometry is quite close to cubic symmetry, this interaction would split the ground state into two groups (a quintet and a septet) of quasidegenerate levels. However, the magnitude of the splitting required to explain this anomaly would be at least 1 order of magnitude larger than for other Np^{6+} systems such as NpF_6.[40] Therefore, the Γ_7 doublet should remain degenerate.

As for the hypothesis of a Γ_7^t or Γ_6^t doublet lying 14 cm^{-1} above the Γ_7 ground state, it would require a complete reevaluation of the spectroscopic data and calculations of Bickel et al.,[38,41] according to which the Γ_7 ground state is well-isolated.[38] Indeed, Bickel et al. performed electronic spectroscopy on Na_4NpO_5 at 77 K, and reported four bands in the near-infrared region at 5910, 7225, 8375, and 10 124 cm^{-1},[38] which they assigned to the Γ_7^t and Γ_6^t levels, and two nearest doublets of the $^2F_{7/2}$ levels (Γ_7' and Γ_6'). Besides, the latter scenario, which corresponds to a quasiquartet, is not consistent with the observed small value of the effective paramagnetic moment.

Therefore, the physical origin of 14 cm^{-1} splitting remains unclear. Our findings nevertheless bring new insights into the complex electronic structure of this $5f^1$ system, and point to the need for theoretical calculations to elaborate on our results. New crystal-field investigations would be required to confirm the assignment of Bickel et al. Moreover, the possibility of a splitting of the Γ_7 ground state doublet by yet another phenomenon, such as short-range ordering along the magnetic chains, should also be investigated.

CONCLUSIONS

The present study has used the powerful combination of X-ray diffraction and Mössbauer spectroscopy for the investigation of ternary alkali neptunium oxide crystal structures at a very detailed level. The structures of Na_4NpO_5 and Na_5NpO_6 have been refined for the first time in this work using the Rietveld method. Na_4NpO_5 crystallizes in the tetragonal system and space group $I4/m$, with cell parameters a = 7.535(3) Å, c = 4.616(3) Å, while Na_5NpO_6 adopts monoclinic symmetry, in the space group $C2/m$, with the following cell parameters: a = 5.829(3) Å, b = 9.996(3) Å, c = 5.757(3) Å, and β = 110.73(1)°. The fitted Mössbauer parameters, i.e., quadrupole coupling constants and asymmetry parameters, have been related to the local structural properties around the neptunium ion, as inferred from the X-ray refinements. The Np(VI) and Np(VII) valence states in Na_4NpO_5 and Na_5NpO_6 have moreover been confirmed by the values of the isomer shifts obtained by Mössbauer spectroscopy, i.e., $\delta_{IS}(Na_4NpO_5)$ = −53.5(3) mm $s^{-1}/NpAl_2$ and $\delta_{IS}(Na_5NpO_6)$ = −74.8(3) mm $s^{-1}/NpAl_2$.

Magnetic susceptibility measurements carried out on Na_4NpO_5 have confirmed paramagnetic behavior over the entire temperature range, and Curie−Weiss law constants were derived as $C = 6.92(2) \times 10^{-2}$ emu K mol^{-1} and θ_P = −15.6(3) K, yielding μ_{eff} = 0.74(4) μ_B for the effective moment. Finally, specific heat measurements performed on Na_4NpO_5 at low temperatures have revealed the existence of a Schottky-type anomaly around 7 K. The excess electronic entropy associated with the anomaly was estimated at 4.57 J K^{-1} mol^{-1}. Simulation using a homemade Fortran code has shown that two low lying electronic states with the same degeneracy and separated by 14 cm^{-1} could reproduce the experimental results quite well. Our experimental results have brought new insights into the complex electronic structure in this compound, and point to the need for theoretical calculations to elaborate on our results.

ASSOCIATED CONTENT

Supporting Information

X-ray crystallographic files in CIF format. Selected bond lengths for Na_4NpO_5. High temperature X-ray diffraction studies of Na_4NpO_5 and Na_5NpO_6. Correlation diagram for the Mössbauer data. Comments on the magnetic ordering behavior of Li_4NpO_5. Asymmetric profile shape of Na_4NpO_5 shown in detail. This material is available free of charge via the Internet at http://pubs.acs.org.

AUTHOR INFORMATION

Corresponding Authors

*E-mail: als77@cam.ac.uk.
*E-mail: philippe.raison@ec.europa.eu.

Author Contributions

A.L.S. and A.H. contributed equally to this work.

Notes

The authors declare no competing financial interest.

ACKNOWLEDGMENTS

The authors would like to express their gratitude to D. Bouëxière and G. Pagliosa for the collection of room temperature and high temperature X-ray diffraction data. A.L.S. acknowledges the European Commission and the Ras al Khaimah Centre for Advanced Materials for funding her Ph.D. studentship.

REFERENCES

(1) *2009 GIF R&D Outloook for Generation IV Nuclear Energy Systems*; INIS-FR-11-0958; 2009.
(2) Keller, C.; Koch, L.; Walter, K. H. *J. Inorg. Nucl. Chem.* **1965**, *27*, 1205−1223.
(3) Keller, C.; Koch, L.; Walter, K. H. *J. Inorg. Nucl. Chem.* **1965**, *27*, 1225−1232.
(4) Smith, A. L.; Raison, P. E.; Konings, R. J. M. *J. Nucl. Mater.* **2011**, *413*, 114−121.
(5) Bickel, M.; Kanellakopulos, B. *J. Solid State Chem.* **1993**, *107*, 273−284.

DOI: 10.1021/acs.inorgchem.5b00462
Inorg. Chem. 2015, 54, 4556−4564

(6) Kalvius, G. M.; Dunlap, B. D.; Asch, L.; Weigel, F. *J. Solid State Chem.* **2005**, *178*, 545−553.
(7) Yoshida, Z.; Johnson, S. G.; Kimura, T.; Krsul, J. R. In *The Chemistry of the Actinide and Transactinide Elements*; Morss, L. R., Edelstein, N., Fuger, J., Katz, J. J., Eds.; Springer: New York, 2006; pp 699−812.
(8) Santini, P.; Carretta, S.; Amoretti, G.; Caciuffo, R.; Magnani, N.; Lander, G. H. *Rev. Mod. Phys.* **2009**, *81*, 807−864.
(9) Dickson, D. P. E.; Berry, F. J. *Mössbauer Spectroscopy*; Cambridge University Press: New York, 2005.
(10) Smith, A. L.; Colineau, E.; Griveau, J.-C.; Raison, P.; Konings, R. J. M. *J. Chem. Thermodyn.* **2015**, submitted.
(11) Unger, L. M.; Trubey, D. K. *Specific Gamma-Ray Dose Constants for Nuclides Important to Dosimetry and Radiological Assessment*; ORNL/RSIC-45/RI, 1982
(12) Rodriguez-Carvajal, J. *Physica B* **1993**, *192*, 55−69.
(13) Taylor, D. *Br. Ceram. Trans. J.* **1984**, *83*, 5−9.
(14) Lashley, J. C.; et al. *Cryogenics* **2003**, *43*, 369−378.
(15) Javorský, P.; Wastin, F.; Colineau, E.; Rebizant, J.; Boulet, P.; Stewart, G. *J. Nucl. Mater.* **2005**, *344*, 50−55.
(16) Roof, I. P.; Smith, M. D.; zur Loye, H.-C. *J. Cryst. Growth* **2010**, *312*, 1240−1243.
(17) Morss, L.; Appelman, E.; Gerz, R.; Martin-Rovet, D. *J. Alloys Compd.* **1994**, *203*, 289−295.
(18) Smith, A. L.; Raison, P. E.; Martel, L.; Charpentier, T.; Farnan, I.; Prieur, D.; Hennig, C.; Scheinost, A.; Konings, R. J. M.; Cheetham, A. K. *Inorg. Chem.* **2014**, *53*, 375−382.
(19) Shannon, R. D. *Acta Crystallogr., Sect. A* **1976**, *32*, 751−767.
(20) Morss, L. R.; Appelman, E. H.; Gerz, R. R.; Martin-Rovet, D. *J. Alloys Compd.* **1994**, *203*, 289−295.
(21) Keller, C. In *Inorganic Chemistry, ser. 1. 7*; Bagnall, K., Ed.; Butterworths: London, 1972, p479.
(22) Smith, A. L. Unpublished results, 2015
(23) Jové, J.; Cousson, A.; Abazli, H.; Tabuteau, A.; Thévenin, T.; Pagès, M. *Hyperfine Interact.* **1988**, *39*, 1−16.
(24) Jové, J.; Proust, J.; Pagès, M.; Pyykkö, P. *J. Alloys Compd.* **1991**, *177*, 285−310.
(25) Nectoux, F.; Jové, J.; Cousson, A.; Pagès, M.; Gal, J. *J. Magn. Magn. Mater.* **1981**, *24*, L113−L116.
(26) Cordfunke, E. H. P.; IJdo, D. J. W. *J. Solid State Chem.* **1995**, *115*, 299−304.
(27) Jové, J.; Cousson, A.; Gasperin, M. *Hyperfine Interact.* **1986**, *28*, 853−856.
(28) Hinatsu, Y.; Doi, Y. *J. Solid State Chem.* **2006**, *179*, 2079−2085.
(29) Tabuteau, A.; Pagès, M. In *Handbook on the Physics and Chemistry of the Actinides*; Freeman, A. J., Lander, G. H., Eds.; Elsevier: New York, 1985; Vol. 3, Chapter 4, p 185.
(30) Friedt, J. M.; Shenoy, G. K.; Pagès, M. J. *Phys. Chem. Solids* **1978**, *39*, 1313−1316.
(31) He, L.; Jové, J.; Proust, J.; Pagès, M. ^{237}*Np Mössbauer Spectroscopy of Some Ionic Hepta and Hexavalent Oxoneptunates*; 19ème Journées des Actinides, Madonna di Campiglio, Italy, 1989; p 11.
(32) Scholder, R. *Angew. Chem.* **1958**, *70*, 583−614.
(33) Wolf, R.; Hoppe, R. *Z. Anorg. Allg. Chem.* **1985**, *528*, 129.
(34) Hauck, J. *Z. Naturforsch. Teil B.* **1968**, *23*, 1603−1603.
(35) Bickel, M.; Kanellakopulos, B.; Appel, H.; Haffner, H.; Geggus, S. *J. Less-Common Met.* **1986**, *121*, 291−299.
(36) Fröhlich, K.; Gütlich, P.; Keller, C. *J. Chem. Soc., Dalton Trans.* **1972**, 971−974.
(37) Friedt, J. M. *Radiochim. Acta* **1983**, *32*, 105−127.
(38) Bickel, M.; Kanellakopulos, B.; Powietzka, B. *J. Less-Common Met.* **1991**, *170*, 161−169.
(39) Swalin, R. A. *Thermodynamics of Solids*, 1st ed.; John Wiley & Sons: New York, 1962.
(40) Dunlap, B. D.; Kalvius, G. M. In *Handbook on the Physics and Chemistry of the Actinides, Vol. 2*; Freeman, A. J., Lander, G. H., Eds.; Elsevier: Amsterdam, 1985; pp 71−86.
(41) Kanellakopulos, B.; Keller, C.; Klenze, R.; Stollenwerk, A. H. *Physica B.* **1980**, *102*, 221−225.

DOI: 10.1021/acs.inorgchem.5b00462
Inorg. Chem. 2015, 54, 4556−4564